

Modification of Graphite Surface by Intense Pulsed Ion-beam Irradiation

Kenji Kashine* Member

Hisayuki Suematsu* Member

Weihua Jiang* Member

Kiyoshi Yatsui* Member

Surface modification has been carried out of graphite targets irradiated by intense pulsed ion beam. The highly oriented pyrolytic graphite (HOPG) targets were irradiated by 70 – 120 J/cm² of pulsed ion beams. To evaluate temperature on the irradiated surface, the deposited energy was measured by using the thermistors attached on the back of the targets. The fast heating and fast quenching occurred on the target surface, which were enhanced at the higher energy density of beam irradiation. On the irradiated surfaces, sphere particles and whiskers were found by scanning electron microscope observations. By Raman spectroscopy, structural changes were confirmed on the irradiated surfaces and the intensity ratio of a peak at 1360 cm⁻¹ to that at 1580 cm⁻¹ was increased with increasing the ion beam energy density.

Keywords : pulsed ion beam, high-density ablation plasma, surface modification, Raman spectroscopy

1. Introduction

It is widely known that there are many allotropes of carbons, such as graphite, diamond and diamond-like-carbon (DLC). Their physical properties are strongly dependent on the ratio of sp^2 (graphite-like) and sp^3 (diamond-like) bonds. The ratio varies with synthesizing conditions including the pressure and the temperature. Not only synthesis of the bulk samples, but also modification of the bulk surface of the carbon have been carried out by shock wave⁽¹⁾, pulsed laser irradiation⁽²⁾⁽³⁾ and ion irradiation.

In the ion irradiation method, the irradiated ions can travel only a very short distance in the target due to strong interaction with matter. This distance is called the range. For instance, the range is only ~13 μm for the proton with the energy of 1 MeV in a carbon target. Being dependent on the ion-beam energy density deposited, the ion irradiation can be divided into two processes for modifying the graphite surface, i.e. ion implantation and ion-beam ablation. In the ion implantation, the ion flux of approximately $10^7\sim 10^{10}$ ions/(cm²·s) were applied on the graphite target, where the lattice damage was observed in the target⁽⁴⁾. On the other hand, by applying an intense pulsed ion beam, it is easily possible to raise the temperature above a melting point of the target. The heated surface layer turns into a high-density ablation plasma⁽⁵⁾. And then, the target surfaces can be heated and the pressure wave propagates in the target.

In our previous works, we have studied the kinetics of the aluminum targets by the pulsed ion-beam irradiation⁽⁶⁾⁻⁽⁸⁾. From these works, we have found experimentally and analytically that not only temperature but also pressure of the ablation plasma were enhanced at the higher energy density of the ion beam irradiation. Thus, it may be possible to control the pressure and the temperature in the targets, and we expect the surface modification of the target materials. The temperature or pressure effect of the

target materials using the pulsed ion beam has recently attracted considerable attention in the field of surface modification. Preliminary data on the surface modification of graphite by the pulsed ion beam irradiation was reported by the present authors, but the temperature of the target was not studied.

In this paper, we attempted the surface modification of graphite targets by the pulsed ion beam irradiation. The highly oriented pyrolytic graphite (HOPG) targets were irradiated by the ion beams with energy density of 70 – 120 J/cm². To evaluate the surface temperature at the instance of the ion-beam irradiation, a thermal energy deposited into the target was measured by the thermistor. The carbon ablation plasma was observed by an ultra high-speed camera. The morphology of the irradiated surface was observed by a scanning electron microscopy (SEM). The structure of the irradiated targets was investigated by a Raman spectroscopy.

2. Experimental Setup

2.1 Ion Beam Diode The ion-beam irradiation experiments were carried out in a pulsed power generator, "ETIGO-II"⁽⁹⁾. Figure 1 illustrates the outline of the experimental setup using a magnetically insulated ion-beam diode (MID)⁽¹⁰⁾. The diode consisted of the anode (inner electrode) and the cathode (outer electrode). The concave-shaped anode had a flashboard (polyethylene) on its surface. The cathode had slits to extract the ion beam. In addition, the cathode acted as a one-turned theta-pinch coil, where the current was supplied by an external power supply of a capacitor bank. The current in the cathode generated an insulating magnetic field in the gap between the cathode and the anode, by which the electrons emitted from the cathode were prevented from arriving at the anode. On the other hand, the ions (approximately 75% proton) are accelerated toward the cathode and focused toward the geometric focusing point ($d_{AT} = 160$ mm) through a vane-structure cathode. The peak voltage of the diode was 1.1 MV. The pulse width was approximately 60 ns. The diode and the target chambers were evacuated to 2×10^{-4} Torr of pressure during the experiments.

* Extreme Energy-Density Research Institute, Nagaoka University of Technology
1603-1 Kamitomioka, Nagaoka 940-2188

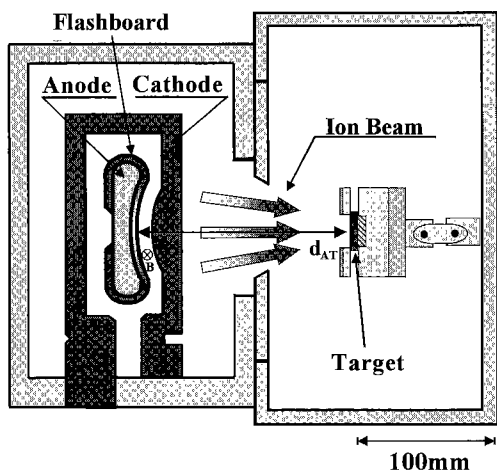


Fig. 1. Experimental setup using a magnetically insulated ion-beam diode (MID)

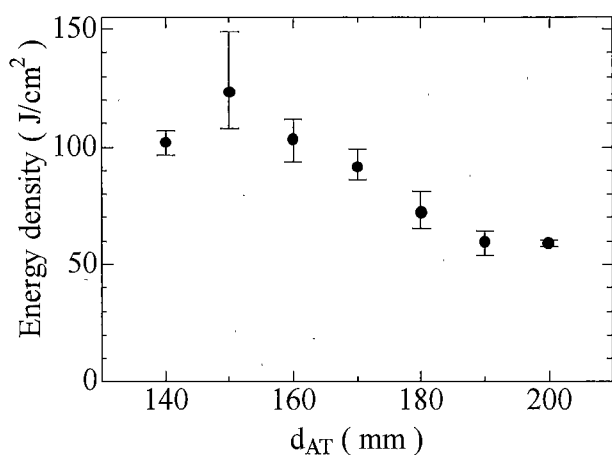


Fig. 2. Ion-beam energy density as a function of anode-target distance

The ion-beam energy density was measured by a calorimeter at various distance between the anode and the target material (d_{AT}). Figure 2 shows the average energy density as a function of d_{AT} . The maximum average energy density of $\sim 120 J/cm^2$ was obtained at $d_{AT} = 150$ mm, which is 10 mm closer than the geometric focal point due to a self magnetic field. The energy density is decreased at $d_{AT} > 150$ mm.

2.2 Deposited Energy Measurement Figure 3 illustrates the schematic of the deposited energy measurement by using the thermistor. The HOPG (Advanced Ceramics Corporation, Grade ZYH) plates with thickness of 1 mm was used for the target. The physical properties of the HOPG were shown in Table 1. The temperature rise of the target (ΔT) was measured by the thermistor (SYE-64: Technol Seven Co.). The thermistor was placed on the backside of the HOPG target. The target was located behind an aperture (8 mm ϕ). The deposited energy Q (J) into the target is given by

$$Q = mC \Delta T \quad (1)$$

where m (g) is the mass of the target and C (J/(K·g)) the specific heat of the target (0.7 J/(K·g) for carbon). The deposited energy per unit area H (J/cm 2) is given by

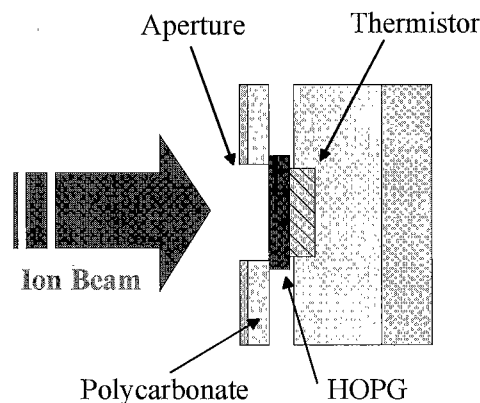


Fig. 3. Schematic to measure the deposited energy on a carbon target

Table 1. Physical properties of the HOPG

Highly oriented pyrolytic graphite (HOPG)	
Size	10mm×10mm×1mm
Density	2.26 g/cm 3
Thermal conductivity	0.08 W/(cm·K) (\perp (002))
Thermal diffusivity	0.05 cm 2 /s

$$H = Q/S \quad (2)$$

where S (cm 2) is the irradiated area. The time evolution of the ablation plasma was observed by a high-speed camera (NAC Inc., ULTRA-NAC). The photographs were taken with the exposure time of 30 ns and the inter-frame of 500 ns.

2.3 Surface Modification In the surface modification experiments, the HOPG targets were irradiated by the ion beams with energy density of 70~120 J/cm 2 . One of the targets was set parallel to the cathode, and d_{AT} was changed at 150 and 180 mm. The number of shots for each target was one. The morphology of the ablated surfaces was observed by a scanning electron microscope (JEOL, JSM-6700F). The Raman spectra were obtained using a Model Labram Infinity spectroscop (Jobin Yvon Co.), in a backscattering mode using an argon-ion laser with the wavelength of 514.5 nm at a power of 10 mW.

3. Experimental Results and Discussions

3.1 Evaluation of Temperature on the Target Surface

Figure 4 shows typical high-speed photographs of the ablation plasma, where the HOPG target was irradiated by $\sim 70 J/cm^2$ of the ion beam. The HOPG target was placed in the absence of the aperture on the target holder. The ion beam irradiates the target from the right-hand side. We observed the plasma light on the target surface for approximately 1 μ s after the beam irradiation.

Figure 5 shows the time evolution of the deposited energy on the HOPG targets. Here, the HOPG targets were placed at $d_{AT} = 160$ and 180 mm, where the ion beams with ~ 100 and $\sim 70 J/cm^2$ of the energy density were irradiated on the targets, respectively. The time of zero in Fig. 5 corresponds to the start of the beam irradiation on the target. The maximum deposited energy (Q) of 0.8 and 0.6 J was obtained with each condition. Thus, the deposited energy per unit area (H) were estimated to be 1.6 and 1.3 J/cm 2 , respectively. Since the ablated area on the target has been observed to be same as the target size, and the targets were

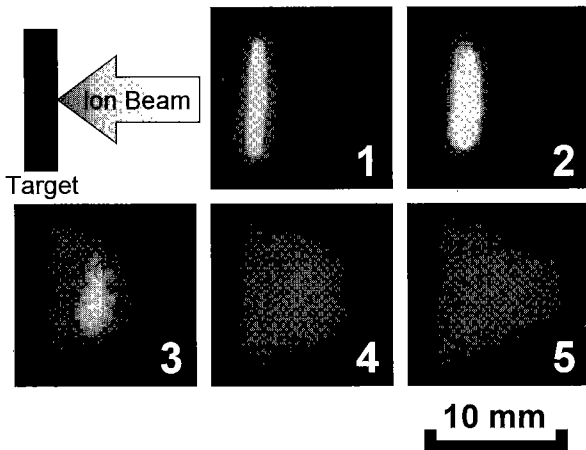


Fig. 4. High-speed photographs of the carbon plasma formed by $\sim 70 \text{ J/cm}^2$ of ion beam irradiation at $d_{AT} = 180 \text{ mm}$. Here, the exposure time and inter-frame are 30 ns and 500 ns, respectively

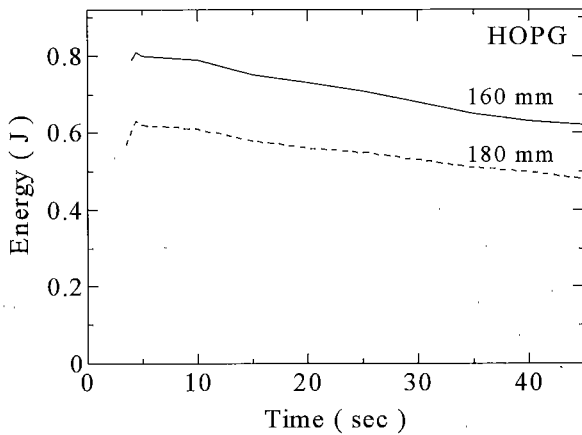


Fig. 5. Time evolution of deposited energy on the HOPG targets

used always flat and thin plates, the heat diffusion in the targets can be considered to be one-dimensional. Assuming the heat diffusion from the ablation plasma being constant during the period τ (sec), the heat flux F_0 (W/cm^2) is given by

$$F_0 = H / \tau \dots\dots\dots (3)$$

In Fig.4, the strong light emission of the ablation plasma on the target surface was observed for approximately $1 \mu\text{s}$, being correspond to τ . Assuming the target was deposited by the thermal energy for the duration of $1 \mu\text{s}$, we obtained the heat flux (F_0) of 1.6×10^6 and $1.3 \times 10^6 \text{ W/cm}^2$ for $d_{AT} = 160$ and 180 mm samples, respectively.

In the one-dimensional heat diffusion in the direction perpendicular to the target surface, the surface temperature T ($^\circ\text{C}$) can be evaluated by following equations⁽¹¹⁾⁽¹²⁾,

$$T(t) = \frac{2F_0}{K} \sqrt{\frac{\kappa}{\pi}} t \quad \text{for } 0 < t < \tau \dots\dots\dots (4)$$

$$T(t) = \frac{2F_0}{K} \sqrt{\frac{\kappa}{\pi}} (\sqrt{t} - \sqrt{t-\tau}) \quad \text{for } t > \tau \dots\dots\dots (5)$$

where K is the thermal conductivity ($\text{W/(cm}\cdot\text{K)}$) and κ the thermal diffusivity (cm^2/s).

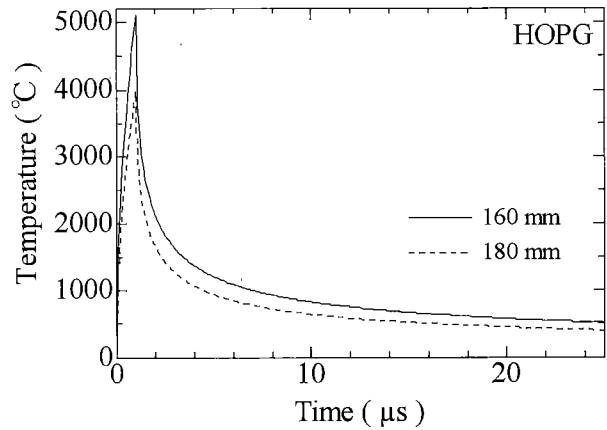


Fig. 6. Time evolution of the target surface temperature

Substituting the present conditions into eqs. (4) and (5), we obtained the time evolution of the surface temperature as shown in Fig. 6. We see the target surfaces were quickly heated by the ablation plasma, and then quenched. In the phase diagram of carbon, the phase change between solid and liquid phase exist at $\sim 5000^\circ\text{C}$. Therefore, at $d_{AT} = 160 \text{ mm}$, it is expected that the surface of solid graphite changes to liquid phase graphite by the ablation plasma. The structural changes will be expected by these thermal effects.

3.2 Surface Modification of Graphite Targets by Ion Beam Irradiation

Figure 7 shows SEM images of the surface of (a) unirradiated, (b) irradiated HOPG targets and (c) the magnified image of the point P in Fig. 7(b). The irradiated sample was placed at $d_{AT} = 150 \text{ mm}$, where the ion beams with $\sim 120 \text{ J/cm}^2$ of energy density were irradiated on the target. The observed area was the center of the irradiated region on the target surface. From Fig. 7(b) and (c), the irradiated sample has many sphere particles and whiskers. The diameter of these particles was approximately $0.5\text{--}1 \mu\text{m}$. The surface morphology of other samples which was irradiated at $d_{AT} = 180 \text{ mm}$ were similar to that of Fig. 7(b). Figure 8 shows the cross sectional view of the irradiated HOPG target. The cavitory whiskers were clearly observed on the irradiated target surface.

The growth mechanism of the metallic whisker from solids was studied by many scientists. Furuta *et al.*⁽¹³⁾ studied the growth of Sn whiskers from a solid Al-Sn alloy. The whiskers were formed by growing a topmost grain in the strained alloy. Fisher⁽¹⁴⁾ and Hasinguti⁽¹⁵⁾ observed the growth of whiskers from solid Sn plated Zn samples. The growth rate was increased with increasing applied pressure by exerted in tightening the clamp. In the present experiment of the intense pulsed ion beam irradiation on the graphite target, carbon whiskers were observed to be present (Fig. 7(b)). Although, as far as the present authors know, no results have been reported on the growth of carbon whiskers from solid, it is likely that the growth of carbon whiskers will be enhanced by the hydraulic pressure. Hence, the presence of the carbon whiskers observed in Fig. 7 (b) on the pulsed ion beam irradiation on the graphite targets may give us an evidence of the generation of hydraulic pressure, which had been numerically predicted by the previous studies.

The structure of the irradiated targets was investigated by the Raman spectroscopy. Figure 9 shows the typical Raman spectra of the irradiated targets. The HOPG targets were placed at $d_{AT} = 150$ and 180 mm , where ion beams with ~ 120 and $\sim 70 \text{ J/cm}^2$ of

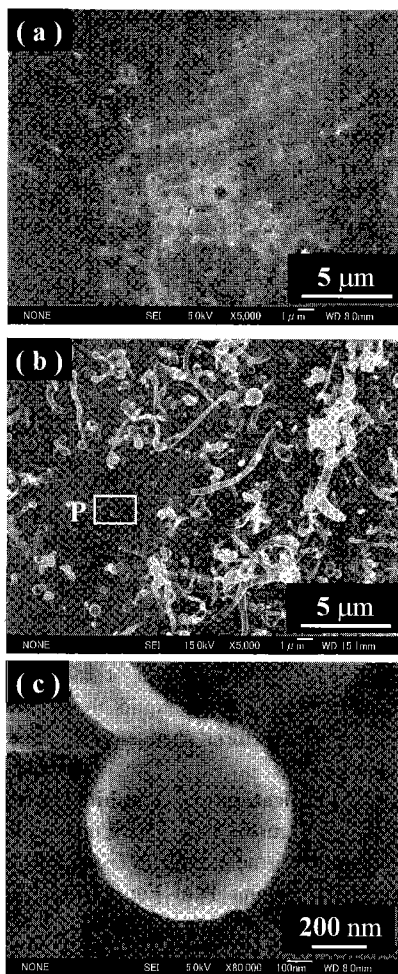


Fig. 7. Surfaces of (a) unirradiated, (b) irradiated HOPG targets observed by SEM, (c) is the magnified image of point P in Fig. 7(b)



Fig. 8. Cross sectional view of the irradiated HOPG target observed by SEM

energy density were irradiated on the targets, respectively. The observed area was the center of the irradiated region. In the unirradiated target, the sharp peak can be observed in the spectrum at $\sim 1580 \text{ cm}^{-1}$, called *G* peak. The *G* peak corresponds to an in-plane vibration of graphite structure (E_{2g}), which indicates the presence of sp^2 bonds. In the irradiated target, the broad peak can be observed in the spectrum at $\sim 1360 \text{ cm}^{-1}$, called *D* peak. The *D* peak, corresponds to the structural defects in graphite⁽¹⁶⁾. The FWHM and the ratio of the peak intensity of those peaks give us the information about the microstructure of the carbon material. After the beam irradiation, the FWHM values of *G* and *D* peaks

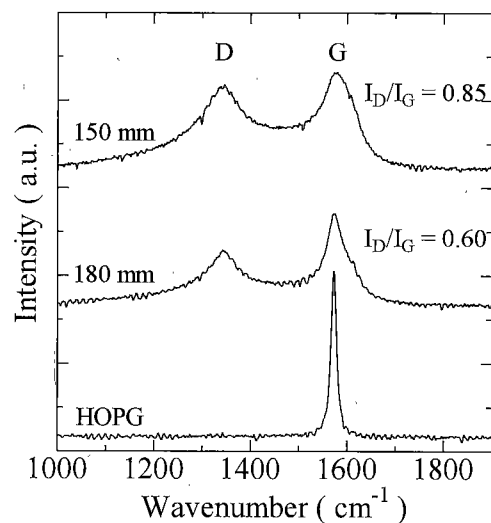


Fig. 9. Raman spectra of the unirradiated and irradiated HOPG targets placed at $d_{AT} = 150 \text{ mm}$ and 180 mm

are broadened and that the intensities of *D* peak are enhanced. On the Raman spectra of the graphite, many scientists have studied the relation between the peak shift of the *D* or *G* peaks and disordering of the crystal structure⁽¹⁷⁾⁻⁽¹⁹⁾. In our experiments, however, no peak shift could be observed.

The intensity ratio of *D* peak to *G* peak (I_D/I_G) is very important because it indicates the degree of disordering. In the present experiment, the intensity ratio of I_D/I_G is clearly increased with increasing the ion-beam energy density. Thus, the degree of disordering is enhanced at the higher energy density.

The result of the SEM and Raman spectroscopy analysis, it is suggested that the pressure and temperature generated by the ablation plasma is influenced by the beam irradiated targets. The above consideration can be supported by the presence of the whiskers on the irradiated surface and the structural changes in HOPG target investigated by the Raman spectroscopy. It is possible to modify the surface structure at the higher energy density of beam irradiation.

4. Conclusions

The surface modification of the highly oriented pyrolytic graphite (HOPG) targets have been carried out by the pulsed ion-beam irradiation. To evaluate the irradiated surface temperature, the deposited energies with the ablation-plasma radiation on the HOPG targets were measured. The maximum deposited energy was obtained to be 0.8 J with 100 J/cm^2 of the ion-beam irradiation. The fast heating and fast quenching effects were observed on the target surface, and these effects can be enhanced at the higher energy density of beam irradiation.

In the SEM analysis, sphere particles and whiskers which approximately $0.5\text{--}1 \text{ }\mu\text{m}$ in diameter were observed on the irradiated surface. These whiskers may be grown under the hydraulic pressure by the ablation-plasma radiation. In the Raman spectra, we see the intensity ratio of I_D/I_G was increased with increasing the ion-beam energy density. These results suggested us that the pressure and temperature effects provided by the ablation plasma were valid on the surface modification of the graphite targets by pulsed ion beam irradiation. We have found

the ablation plasma produced by the intense pulsed ion-beam irradiation can be used for the surface modification of the target materials.

Acknowledgements

This work was partly supported by the Grant-in-Aid for Scientific Research and the 21st. Century COE Program of the Ministry of Education, Culture, Sports, Science and Technology of Japan.

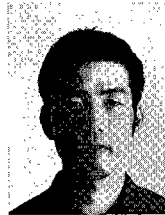
(Manuscript received March 27, 2003, revised July 30, 2003)

References

- (1) K. Yamada and Y. Tanabe. "Shock-induced phase transition of oriented pyrolytic graphite to diamond at pressures up to 15 GPa", *Carbon*, Vol.40, pp 261-269 (2002)
- (2) A. Mechler, P. Heszler, Zs. Marton, M Kovacs, T. Szorenyi, and Z. Bor: "Raman spectroscopic and atomic force microscopic study of graphite ablation at 193 and 248 nm", *Appl. Surf. Sci.*, Vol.154-155, pp.22-28 (2000)
- (3) M. D. Shirik and P. A. Molian: "Ultra-short pulsed laser ablation of highly oriented pyrolytic graphite", *Carbon*, Vol.39, pp.1183-1193 (2001)
- (4) B. S. Elman, M. Shayegan, M. S. Dresselhaus, H. Mazurek, and G. Dresselhaus: "Structural characterization of ion-implanted graphite", *Phys. Rev. B*, Vol.25, pp.4142-4156 (1982)
- (5) K. Yatsui: "Industrial applications of pulsed power and particle beams", *Laser and Part. Beams*, Vol.7, pp.733-741 (1989)
- (6) K. Yatsui, H. Shinkai, K. Kashine, W. Jiang, M. Kagihiro, and N. Harada: "Foil acceleration by intense pulsed ion beam ablation plasma", *Jpn. J. Appl. Phys.*, Vol.40, pp 955-959 (2001)
- (7) N. Harada, M. Yazawa, K. Kashine, W. Jiang, and K. Yatsui: "Development of a numerical tool for foil acceleration by an intense pulsed ion beam", *Jpn. J. Appl. Phys.*, Vol.40, pp.960-964 (2001)
- (8) K. Kashine, M. Yazawa, N. Harada, W. Jiang, and K. Yatsui: "Foil acceleration of double-layer target by intense pulsed ion beam ablation", *Jpn. J. Appl. Phys.*, Vol.41, pp.4014-4018 (2002)
- (9) A. Tokuchi, N. Nakamura, T. Kunimatsu, N. Ninomiya, M. Den, A. Araki, K. Masugata, and K. Yatsui "3MV pulse-power generator at the technological university of nagaoka", Proc 2nd Int. Topical Symp. on Inertial Confinement Fusion Research by High-Power Particle Beams, ed. by K. Yatsui, Nagaoka University of Technology, Nagaoka, Japan, pp.430-439 (1986)
- (10) K. Yatsui, A. Tokuchi, H. Tanaka, H. Ishizuka, A. Kawai, E. Sai, K. Masugata, M. Ito, and M. Matsui: "Geometric focusing of intense pulsed ion beams from racetrack type magnetically insulated diodes", *Laser and Part. Beams*, Vol.3, pp.119-155 (1985)
- (11) H. S. Carslaw and J. C. Jaeger: *Conduction of Heat in Solids*, 2nd ed., p.75, Oxford Univ. Press (1959)
- (12) M. Yatsuzuka, Y. Hashimoto, T. Yamasaki, and H. Uchida. "Amorphous layer formation on nickel alloy surface by intense pulsed ion beam irradiation", *Jpn. J. Appl. Phys.*, Vol.35, pp.1857-1861 (1996)
- (13) N. Furuta and K. Hamamura: "Growth mechanism of proper tin-whisker", *Jpn. J. Appl. Phys.*, Vol.8, pp.1404-1410 (1969)
- (14) R. M. Fisher, L. S. Darken, and K. G. Carroll: "Accelerated growth of tin whiskers", *Acta metallurgica*, Vol.2, pp.368-373 (1954)
- (15) R. R. Hasiiguti: "A tentative explanation of the accelerated growth of tin whiskers", *Acta metallurgica*, Vol.3, pp.200-201 (1955)

- (16) R. J. Nemanich and S. A. Solin: "First- and second-order Raman scattering from finite-size crystals of graphite", *Phys. Rev. B.*, Vol.20, pp.392-401 (1979)
- (17) R. O. Dillon, J. A. Woollam, and V. Katkanant: "Use of Raman scattering to investigate disorder and crystallite formation in as-deposited and annealed carbon films", *Phys. Rev. B.*, Vol.29, pp.3482-3489 (1984)
- (18) D. Beeman, J. Silverman, R. Lynds, and M. R. Anderson: "Modeling studies of amorphous carbon", *Phys. Rev. B.*, Vol.30, pp 870-875 (1984)
- (19) A. C. Ferrari and J. Robertson: "Interpretation of Raman spectra of disordered and amorphous carbon", *Phys. Rev. B.*, Vol.61, pp 14095-14107 (2000)

Kenji Kashine



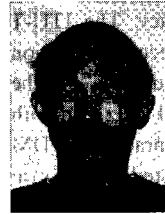
(Member) was born on October 24, 1975. He received a MS degree in Electronic Engineering from Nagaoka Univ. of Technology in 2000. He is presently a research associate of Kagoshima National College of Technology.

Hisayuki Suematsu



(Member) was born on December 25, 1963. He received a Ph. D. degree from Tokyo Institute of Technology in 1991. He is presently an associate professor of Extreme Energy-Density Research Institute at Nagaoka Univ. of Technology. He is a member of Japan Society of Applied Physics.

Weihua Jiang



(Member) was born on February 17, 1962. He received a Ph. D. degree from Nagaoka Univ. of Technology in 1991. He is presently an associate professor of Extreme Energy-Density Research Institute of Nagaoka Univ. of Technology. He is a member of Physical Society of Japan and Japan Society of Applied Physics.

Kiyoshi Yatsui



(Member) was born on November 3, 1939. He received a Ph. D. degree from Osaka Univ. in 1968. He is presently a professor and director of Extreme Energy-Density Research Institute, Nagaoka Univ. of Technology. He is a member of Japan Society of Applied Physics, Laser Society of Japan, APS, and IEEE.